Phase Behavior of Polystyrene-*block*-poly(4-vinylpyridine) Copolymers Coordinated by Metal Chloride

Dong Hyun Lee, Sung Hyun Han, Wonchul Joo, and Jin Kon Kim*

National Creative Research Center for Block Copolymer Self-Assembly, Department of Chemical Engineering and Polymer Research Institute, Pohang University of Science and Technology, Kyungbuk 790-784, Korea

June Huh*

School of Materials Science and Engineering, Seoul National University, Seoul 151-742, Korea

Received October 30, 2007; Revised Manuscript Received January 29, 2008

ABSTRACT: The effect of cadmium chloride ($CdCl_2$) on the phase behavior of polystyrene-*block*-poly(4-vinylpyridine) copolymer (S4VP) was investigated by using rheometry, small-angle X-ray scattering, and transmission electron microscopy. For this purpose, symmetric S4VPs with various molecular weights were prepared by anionic polymerization. We found that with the addition of $CdCl_2$ the order-to-disorder transition of S4VP was significantly increased because of the intermolecular coordination connecting different P4VP block chains. We also studied the change of the domain spacing (D) upon addition of $CdCl_2$ as well as gelation behavior. At a relatively low content of $CdCl_2$ ($\gamma < 6$, where γ is the number of coordinated $CdCl_2$ per chain), D remains unchanged. However, when the amount of $CdCl_2$ increases further, D begins to decrease due to many coordinations of $CdCl_2$ that strongly perturb block copolymer conformation, including many ring closures. Furthermore, it is found that the scaled gelation point increases with increasing molecular weights of S4VP.

1. Introduction

Block copolymers have drawn much attention because of their molecular self-assembly with spatially periodic nanostructures such as lamellae, hexagonally packed cylinders, body-centered-cubic spheres, and bicontinuous gyroids.[1–3] It is well-known theoretically and experimentally that the phase behavior of a block copolymer is described by the block composition (f), the Flory–Huggins interaction parameter (χ), and the total number of the statistical segments (N).[4–8]

Block copolymers containing poly(2-vinylpyridine) or poly(4-vinylpyridine) have been widely employed to develop functional nanomaterials because of the capability of having specific interactions with either organic or inorganic materials.[9–20] Especially, many research groups have extensively studied the phase behavior of polystyrene-*block*-poly(2-vinylpyridine) copolymers (S2VP) and polystyrene-*block*-poly(4-vinylpyridine) copolymers (S4VP).[21–26] Han and co-workers[26] showed that, despite only a different location of a nitrogen atom in the pyridine ring between S2VP and S4VP, χ between PS and P4VP was much larger than that between PS and P2VP. Accordingly, the order-to-disorder transition temperature (T_{ODT}) of S4VP was much higher compared with that of S2VP at a similar molecular weight. This was explained by the stronger polarizability of P4VP in S4VP compared with that of P2VP in S2VP. Also, Ikkla and co-workers[18–20] have extensively studied the phase behavior and microdomain morphology of S2VP and S4VP containing small molecules capable of having hydrogen bonding or ionic interaction with a nitrogen atom in the pyridine ring.

Recently, some research groups investigated the phase behavior of S2VP and S4VP when nanoparticles are selectively sequestered into one of the blocks. For instance, hexagonally packed cylindrical microdomains of neat S4VP were transformed into lamellar microdomains when CdS nanoparticles were incorporated into P4VP microdomains.[15] This occurred because of the increase of effective volume of P4VP microdomains by the addition of the CdS nanoparticles. Other research groups investigated T_{ODT} and morphology of ion-complexed block copolymers.[27–31] Bates and co-workers showed that the complex between lithium ion and poly(ethylene oxide) in polystyrene-*block*-polyisoprene-*block*-poly(ethylene oxide) copolymers increased effectively T_{ODT}, and morphologies were changed.[28,29] Russell and co-workers reported that the orientation of the lamellar microdomains of polystyrene-*block*-poly(methyl methacrylate) copolymer (PS−PMMA) was enhanced along the electric field direction due to the increase of χ arising from the complexation between lithium and PMMA.[30]

Previously, we reported that the addition of cadmium chloride ($CdCl_2$) to S2VP increased the lamellar domain spacing (D) and T_{ODT} because of a significant change in the chain conformation of the block copolymer by the coordination between $CdCl_2$ and the nitrogen atom in the pyridine ring.[32] For instance, D was increased to 1.4 times that of neat S2VP by the addition of cadmium chloride even at very small amount (less than 5 vol %), and T_{ODT} was also significantly increased. This behavior is contrasted with that of S4VP, showing the decrease of D with increasing content of $CdCl_2$. The completely different behavior of D between S4VP and S2VP is due to the different coordination between $CdCl_2$ and the nitrogen in the pyridine: the intramolecular coordination for S2VP and the intermolecular coordination or nonlocal intramolecular coordination for S4VP, as shown in Scheme 1.

Although our previous study demonstrated some interesting phenomena of the domain swelling/shrinking behavior of $CdCl_2$-coordinated S2VP and S4VP, the phase behavior of S4VP was not fully investigated because of some experimental difficulties; for instance, T_{ODT} of neat S4VP investigated in ref 32 was too high to measure T_{ODT} at the experimentally accessible temperature range (up to ∼300 °C). To investigate the phase behavior of S4VP upon addition of $CdCl_2$, we used symmetric S4VPs with four different molecular weights. One of S4VPs remains fully disordered over the entire temperature range, and another

* To whom correspondence should be addressed. E-mail: jkkim@postech.ac.kr or junehuh@snu.ac.kr.

10.1021/ma702403k CCC: $40.75
Published on Web 03/14/2008

Scheme 1. Two Types of Coordination between $CdCl_2$ and Nitrogen Atoms: (a) Intramolecular Coordination for S2VP and (b) Intermolecular Coordination for S4VP

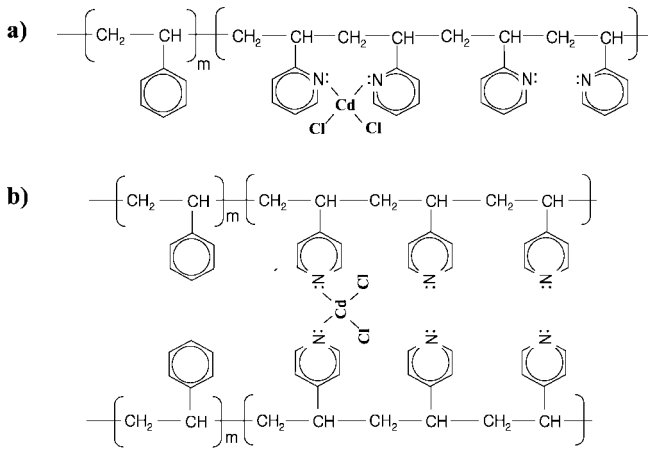

Table 1. Molecular Characteristics of Polystyrene-*block*-poly(4-vinylpyridine) Copolymers Employed in This Study

sample code	M_n	f_{ps}	morphology
S4VP1	5960	0.54	lamellar (T_{ODT} = 268 °C)
S4VP2	3590	0.54	fully disordered
S4VP3	23800	0.52	lamellar (T_{ODT} > 300 °C)
S4VP4	33500	0.52	lamellar (T_{ODT} > 300 °C)

exhibits a T_{ODT} of ~268 °C. The other two become fully ordered state over the entire temperature range.

We found that the T_{ODT} of S4VP increased significantly even at a small amount of $CdCl_2$ because of the intermolecular coordination which therefore induces more contacts between P4VP segments. We also studied the change of D of symmetric S4VP with amount of $CdCl_2$. At a relatively low content of $CdCl_2$, D is nearly unchanged. When the amount of $CdCl_2$ increases further, however, D begins to decrease with increasing content of $CdCl_2$ due to many coordinations of $CdCl_2$ that strongly perturb block copolymer conformation, including many ring closures. Furthermore, theoretical prediction based on the cross-linked system reveals that the gelation point is strongly dependent upon the chain length because of the ring formation in P4VP chains.

2. Experimental Section

Materials. Two symmetric S4VPs (S4VP1 and S4VP2) were synthesized in this laboratory by the anionic polymerization by successive addition of styrene and 4-vinylpyridine monomers in tetrahydrofuran (THF) at −78 °C under argon environment by using *s*-BuLi.[33] The number-average molecular weight (M_n) of S4VP1 and S4VP2 was 5960 and 3590, measured by the ratio of a peak position corresponding to *sec*-butylene initiator and peak positions corresponding to phenyl ring and pyridine ring in the ^1H nuclear magnetic resonance spectrum. Symmetric S4VP3 with M_n = 23 800 and f = 0.52 and S4VP4 with M_n = 33 500 and f = 0.52 were purchased from Polymer Source. Table 1 gives a summary of the molecular weights and block composition as determined by NMR spectroscopy.

S4VP with various amounts of $CdCl_2$ was prepared by mixing THF solution containing S4VP and ethanol with predetermined amount of $CdCl_2$.[32] The molar ratio of $CdCl_2$ to 4VP (p = [$CdCl_2$]/[4VP]) was varied from 0.003 to 0.2. The precipitation of $CdCl_2$ uncoordinated with 4VP units was observed at p > 0.25. Samples for rheology and synchrotron small-angle X-ray scattering (SAXS) were prepared by solution casting and annealed for 48 h under vacuum at 200 °C, except for S4VP2. S4VP2 was annealed for 48 h under vacuum at 140 °C.

Small-Angle X-ray Scattering. SAXS profiles ($I(q)$ vs q (= $4\pi \sin\theta/\lambda$); here, q is the scattering vector and 2θ is the scattering angle) were obtained at beamlines 4C1 and 4C2 at the Pohang Light Source (PLS), Korea.[26,32,33] All samples with a thickness of 1 mm were prepared by compression molding at 160 °C and annealed for 48 h at 200 °C to remove any thermal history. Then, they were sandwiched between two polyimide films to prevent them from flowing at high temperature and put into a heating block under a N_2 environment. The exposure time for all measurements was 100 s. A two-dimensional CCD camera (Princeton Instruments, SCX-TE/CCD-1242) was used to obtain the SAXS intensity. The resulting two-dimensional scattering data were averaged azimuthally to obtain intensity at each q. Then, the scattering intensity was further corrected for the CCD dark current and the scattering from air and two pieces of polyimide films. We found that the contribution of polyimide films on SAXS intensity of the samples was negligible (see Figures S1 and S2 of the Supporting Information).

Oscillatory Shear Rheometry. An Advanced Rheometric Expansion System (TI Instruments) was used in the oscillatory mode with a parallel plate fixture (8 mm diameter). Dynamic temperature sweep experiments under isochronal conditions were conducted to determine the dynamic storage and loss moduli (G' and G'') at a heating rate of 0.5 °C/min up to 300 °C. A strain amplitude of 0.05 and angular frequency of 0.1 rad/s, which lie in the linear viscoelasticity range, were used. The temperature control was satisfactory to within ±1 °C. All experiments were conducted under a nitrogen atmosphere to preclude oxidative degradation of the samples. We found by the gel permeation chromatography that there was no degradation of all of the samples after rheology and SAXS experiment at higher temperatures (see Figure S3 in the Supporting Information).

Transmission Electron Microscopy (TEM). The microdomains of neat S4VPs and S4VPs with various amounts of $CdCl_2$ were investigated by using TEM (S-7600, Hitachi) operating at 120 kV. The specimens were stained with iodine for 2 h at room temperature, which selectively stained the P4VP microdomains. TEM images of specimens were taken at room temperature after a specimen was annealed at 200 °C for 24 h, followed by rapidly quenching to liquid nitrogen. Ultrathin sectioning (50−70 nm) was performed by ultramicrotomy (RMC MT-7000) at room temperature.

3. Results and Discussion

Figure 1a shows the SAXS profiles of S4VP1 at various temperatures. A sharp peak is observed up to 265 °C, and then this peak becomes broad at temperatures higher than 270 °C due to the correlation hole effect. From Figure 1a, we prepared plots of the reciprocal of the maximum scattering intensity ($1/I(q^*)$ with q^* being the scattering angle at the scattering maximum) and the full width at half-maximum of the peak (fwhm) vs the inverse of the absolute temperature ($1/T$), as shown in Figure 1b. The T_{ODT} of S4VP1 was determined to be 268 °C. Figure 2 gives temperature dependence of G' at ω = 0.1 rad/s for S4VP1 with various amounts of $CdCl_2$. A precipitous decrease in G' is referred to as T_{ODT}.[5,34–36] From Figure 2, the T_{ODT} of neat S4VP1 was determined to be 268 °C, which is in good agreement with the T_{ODT} determined from SAXS results as given in Figure 1.

However, when a very small amount of $CdCl_2$ was added in S4VP1, the T_{ODT} increased. For instance, S4VP1[0.003] corresponding to S4VP with the volume fraction of $CdCl_2$ of 0.000 69 has a T_{ODT} at 275 °C, which is 8 °C larger than that of neat S4VP1. Here, the value in brackets after S4VP1 represents the molar ratio of $CdCl_2$ to 4VP, which is the same as the number (p) of coordinated $CdCl_2$ per 4VP monomer unit. We found that S4VP1 with $p \leq 0.004$ becomes a completely disordered state above the T_{ODT}, since the depolarization light intensity becomes a precipitous decrease to zero at the T_{ODT} (see Figure S4 in the Supporting Information). A large increase of the T_{ODT} with increasing amount of $CdCl_2$ is consistent with

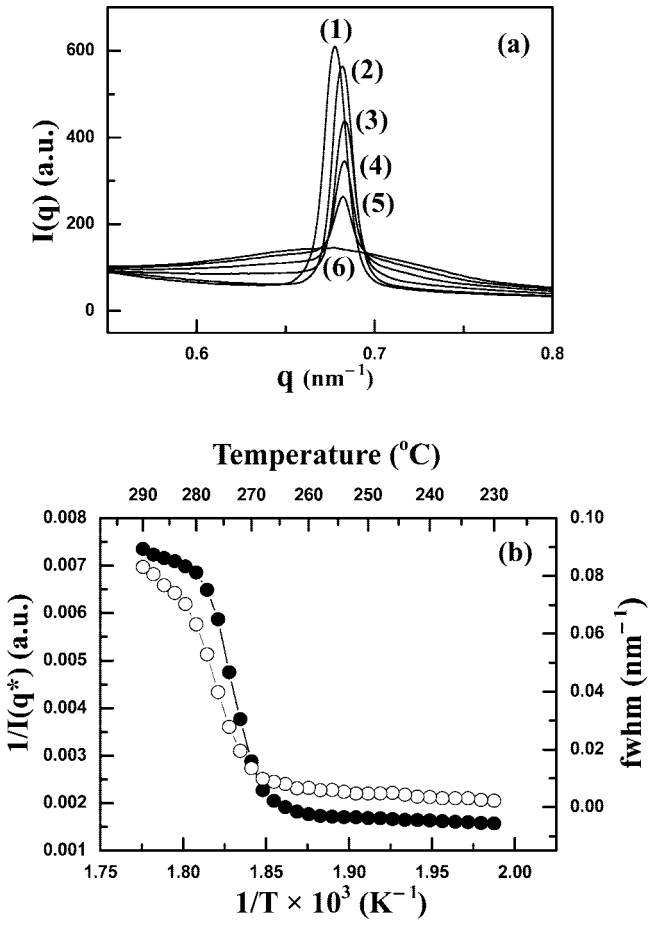

Figure 1. (a) SAXS profiles for neat S4VP1: (1) 240, (2) 260, (3) 268, (4) 270, (5) 272, and (6) 280 °C. (b) Plot of $1/I(q^*)$ (●) and fwhm (○) vs $1/T$ for neat S4VP1.

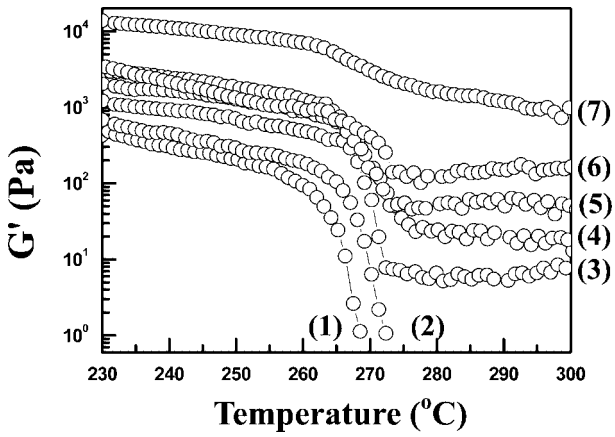

Figure 2. Temperature sweep of G' at $\omega = 0.1$ rad/s for S4VP1 with various amounts of $CdCl_2$: The molar ratio of $CdCl_2$ to 4VP is (1) 0 (neat S4VP), (2) 0.003, (3) 0.005, (4) 0.008, (5) 0.01, (6) 0.02, and (7) 0.05.

results investigated by Balsara and co-workers[37–40] that the T_{ODT} of polystyrene-*block*-polyisoprene copolymer was significantly increased with increasing number of chemical cross-links of PI blocks induced by dicumyl peroxide.

When the amount of $CdCl_2$ was increased further ($p \geq 0.005$), G' decreased near the T_{ODT} of neat S4VP1 but did not change with temperature above 268 °C (see Figure 2). We found that G' for S4VP1 with $p \geq 0.005$ was thermoreversible (see Figures S5 and S6 of the Supporting Information). This behavior of G' with $p \geq 0.005$ is quite different from neat S4VP1 and

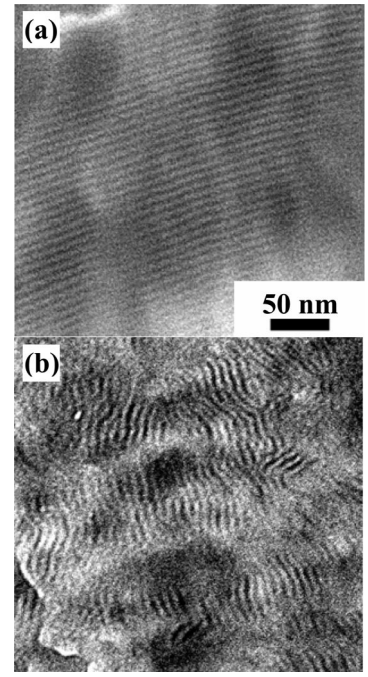

Figure 3. TEM images for S4VP1[0.01] annealed at (a) 240 and (b) 290 °C for 48 h.

S4VP1[0.003]. These results indicate that S4VP1 with higher p exhibits biphasic behavior that some of the lamellar microdomains maintain even at temperatures higher than the T_{ODT}, while others become disordered. The lamellar microdomains can be maintained at a higher temperature due to the coordination of $CdCl_2$ with P4VP chains. Also, with increasing amounts of $CdCl_2$, G' at higher temperatures was gradually increased, indicating that the amount of the remaining lamellar microdomains increases with increasing amount of $CdCl_2$. At a very large amount of $CdCl_2$ (for instance, $p = 0.02$), the decrease of G' near 270 °C is less evident, indicating that almost all of regions are consisted of lamellar microdomains without having disordered state even at 300 °C.

To support the above postulation, TEM experiments were conducted for S4VP1[0.01] annealed at two different temperatures (240 and 290 °C) for 48 h, and the results are shown in Figure 3. S4VP1[0.01] annealed at 240 °C (28 °C lower than the T_{ODT} of net S4VP1) exhibited well-defined lamellar microdomains (Figure 3a). However, S4VP1[0.01] annealed at 290 °C (22 °C higher than the T_{ODT} of S4VP1) showed biphasic behavior, namely two distinct morphologies consisting of lamellar microdomains and disordered phases (Figure 3b). It is noted that the lamellar domain spacing ($D = 2\pi/q^*$) in S4VP1[0.01] annealed at 290 °C looks to be slightly larger than that annealed at 240 °C, although lamellar microdomain structures are not well developed. We also performed depolarized light scattering experiments for S4VP with various amounts of $CdCl_2$, and the results are given in Figure S4 in the Supporting Information. For S4VP1 with $p \leq 0.004$, the intensity precipitously decreased at T_{ODT}, indicating that the samples become completely disorder at high temperatures. For S4VP1 with $0.005 \leq p < \sim 0.01$, the intensity decreased near 285 °C, but it was still larger (not zero corresponding to completely disordered state), suggesting the presence of biphasic behavior at temperatures between 285 and 300 °C. However, at a very high $CdCl_2$ loading (for instance, $p = 0.02$), a strong birefringence intensity was maintained at the entire temperature up to 300 °C, which indicates that a disordered state would not be possible due to many intercoordinations per P4VP chain. Thus, in this situation,

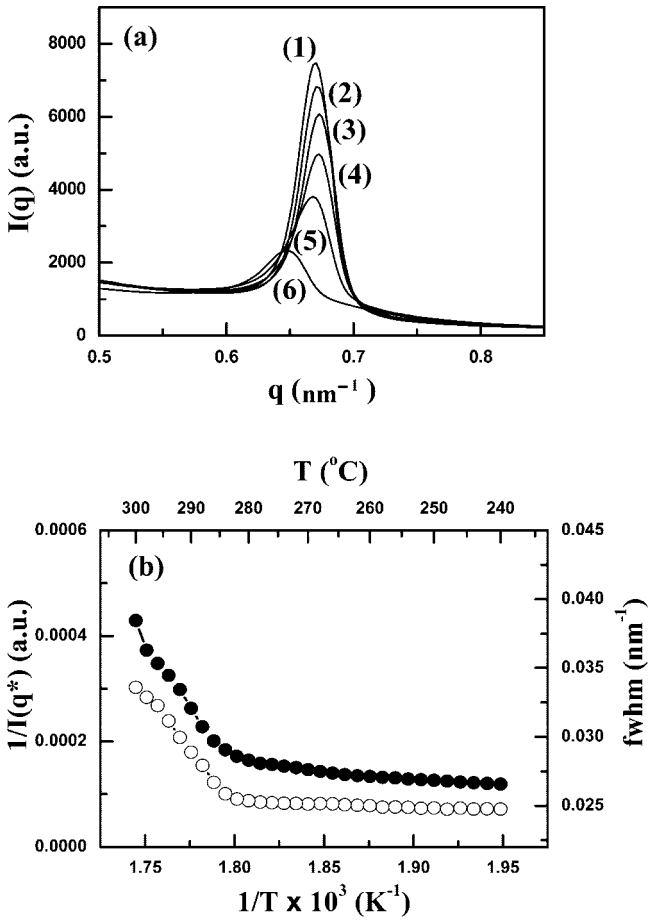

Figure 4. SAXS profiles for (a) S4VP1[0.01] at (1) 260, (2) 270, (3) 280, (4) 285, (5) 290, and (6) 300 °C. (b) Plots of $1/I(q^*)$ vs $1/T$ (●) and plots of fwhm vs $1/T$ (○) for S4VP1[0.01].

a long-range order of lamellar microdomains is just lost without having disordered state.

Figure 4a gives SAXS profiles at various temperatures for S4VP1[0.01]. We found that SAXS profiles are thermoreversible (see Figure S7 in the Supporting Information). $I(q^*)$ decreased gradually up to 280 °C and decreased largely near 282 °C. However, the value of $I(q^*)$ for S4VP1[0.01] even at 300 °C is still large (20 times larger than $I(q^*)$ of neat S4VP1 at disordered state (see Figure 1a). This indicates that S4VP1[0.01] still has microdomains at 300 °C. Figure 4b gives plots of $1/I(q^*)$ and fwhm vs $1/T$ for S4VP1[0.01]. Similarly, fwhm increased moderately (not sharp) near 282 °C compared with Figure 1b where a large increase in fwhm was observed. These results indicate that some of the lamellar microdomains coordinated with $CdCl_2$ still exist even at 300 °C, whereas other lamellar microdomains become disordered near 282 °C. This is consistent with rheological and TEM results given in Figures 2 and 3.

It is seen in Figure 4 that q^* was first shifted to a larger value as S4VP[0.01] underwent the order-to-disorder transition (281 °C), which is a typical behavior of a block copolymer.[5] Interestingly, q^* was shifted to a smaller value when the temperature was further increased to 290 °C, which is an opposite expectation. We speculate that this behavior is attributed to many different chain architectures, for instance, highly interconnecting or ring shape, resulting from the coordination of $CdCl_2$ with P4VP. Since the size (for instance, a radius of the gyration) of a ring polymer is smaller than that of a linear polymer at a given molecular weight, the D of a block copolymer with ring shape becomes smaller. However, with increasing temperature, the degree of the coordination between

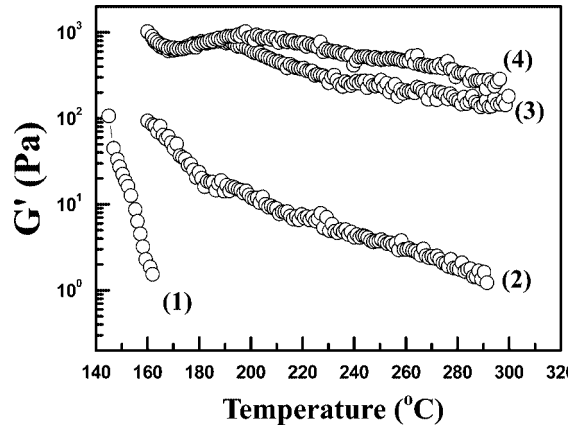

Figure 5. Temperature sweep of G' at $\omega = 0.1$ for S4VP2 with various amounts of $CdCl_2$: (1) neat S4VP2, (2) S4VP2[0.01], (3) S4VP2[0.02], and (4) S4VP2[0.03].

$CdCl_2$ and P4VP decreases, which results in the S4VP chains having less perturbed state. Thus, D would increase (*not decrease*) with increasing temperature at higher temperatures.

Since the coordination of S4VP by $CdCl_2$ could maintain the lamellar microdomains at higher temperatures than the T_{ODT} of neat S4VP, it might be possible to induce microdomains for S4VP exhibiting fully disordered state. Figure 5 gives the temperature sweep of G' at $\omega = 0.1$ rad/s for S4VP2 with various contents of $CdCl_2$. All samples were annealed at 140 °C for 48 h. Neat S4VP2 remains disordered over the entire temperature range. The addition of $CdCl_2$ leads to a significant increase of G'. For S4VP2[0.01] as an example, G' at 160 °C is 100 times larger than that of neat S4VP2. However, S4VP2[0.01] does not show any distinctive birefringence, suggesting that S4VP2[0.01] is still disordered. As the content of $CdCl_2$ increases further (S4VP2[0.02]), G' becomes very large, similar to the situation of S2VP1 with lamellar microdomains, as shown in Figure 2. A distinct birefringence was observed for S4VP2 with $p > 0.02$, revealing that the microdomains were indeed induced by the coordination of $CdCl_2$ with fully disordered S4VP2.

As seen in Figure 6, neat S4VP2 does not exhibit any distinct microdomains, rather microstructures resulting from the concentration fluctuation in the disordered state. On the other hand, S4VP2[0.02] shows lamellar microdomains in some regions, while disordered structures are still seen in other regions. But, S4VP2[0.05] shows microphase-separated microdomains in the entire area. The D of S4VP2[0.05] is larger than that of S4VP2[0.02], although the degree of the ordering is poorer than that of S4VP2[0.02]. The poor ordering might be due to the physical gelation which kinetically prohibits a well-ordered structure. We expect, however, that the ordered lamellar phase even in the highly coordinated system could be thermodynamically stable because the coordination of $CdCl_2$ is in principle breakable; i.e., $CdCl_2$ finds the best coordination sites for the formation of well-ordered lamellar microdomains by breaking and re-forming the physical bonds.

Figure 7 gives SAXS profiles at 140 °C of S4VP2 with various amounts of $CdCl_2$. The neat S4VP2 exhibits a very small peak, indicating the disordered state. Also, the peak intensity of S4VP2[0.01] is still very small, indicating a disordered state. These results indicate that the amount of $CdCl_2$ in S4VP2[0.01] is not enough to induce the lamellar microdomains even though the coordination of $CdCl_2$ with P4VP could increase G'. A similar increase in G' was observed for neat P4VP homopolymer coordinated with $CdCl_2$ (data is not shown). Therefore, a simple increase in G' does not necessarily represent microdomain formation. On the other hand, SAXS profiles of S4VP2[0.02]

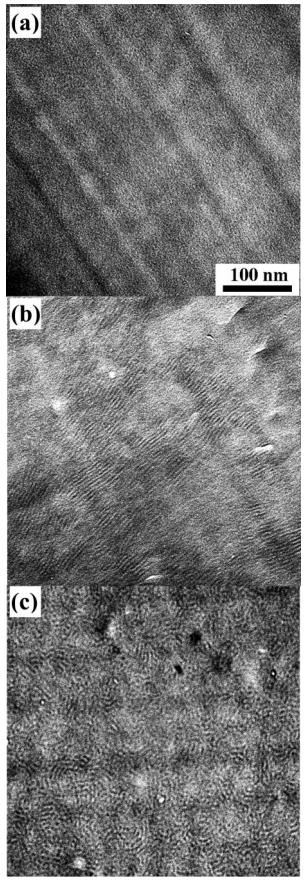

Figure 6. TEM images for (a) neat S4VP2, (b) S4VP2[0.02], and (c) S4VP2[0.05].

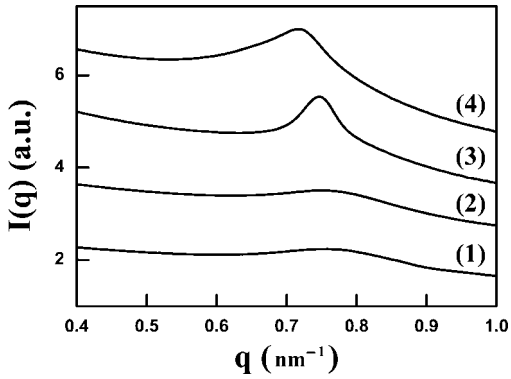

Figure 7. SAXS profiles at 140 °C for (1) neat S4VP2, (2) S4VP2[0.01], (3) S4VP2[0.02], and (4) S4VP2[0.05].

and S4VP2[0.05] show a very distinct first-order peak, indicating that the microphase separation is promoted by the coordination of $CdCl_2$. Interestingly, $I(q^*)$ of S4VP2[0.05] is smaller than that of S4VP2[0.02], though q^* is smaller than that of S2VP2[0.02]. This indicates that the degree of the lamellar microdomain ordering of S4VP2[0.05] is poorer compared with that of S2VP2[0.02], which is consistent with TEM results given in Figure 6.

Figure 8a presents the dependence of D on p for three different S4VPs measured by SAXS profiles. We do not include the data for S4VP2, since neat S4VP2 becomes the disordered state in the entire temperature range. It is seen that D starts to decrease at $p \cong 0.05$ for S4VP3 and $p \cong 0.04$ for S4VP4, whereas D of S4VP1 still remains constant up to $p \cong 0.2$. This result indicates that the number of coordinations needed for severe conformational restriction, which may result in the

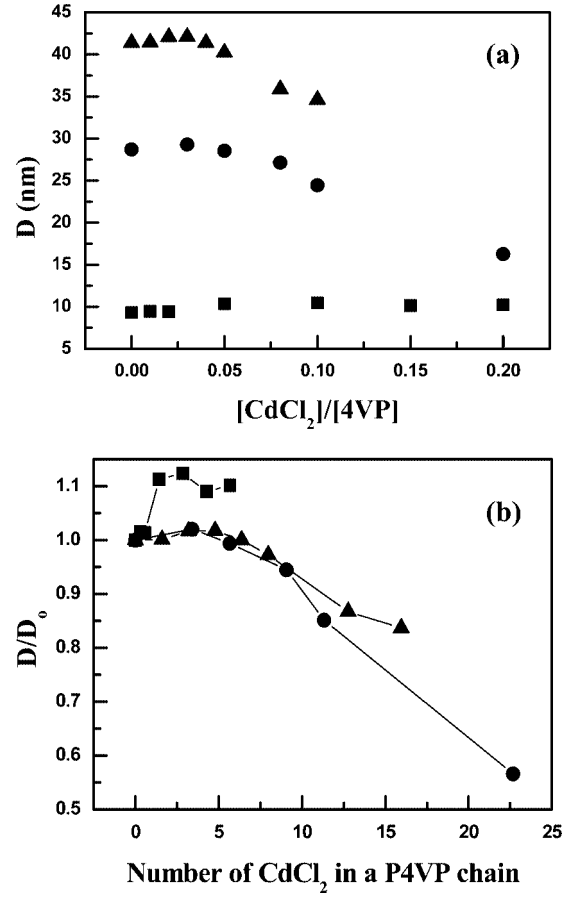

Figure 8. Plots of (a) D vs p and (b) D/D_0 vs γ (the number of $CdCl_2$ per a P4VP chain) for S4VP1 (■), S4VP3 (●), and S4VP4 (▲).

decrease of D, increases with increasing the molecular weight. Obviously, longer chains can have more possibilities of forming longer loops than shorter chains at the same coordination numbers of $CdCl_2$. Thus, γ ($= Np$) rather than p alone would be a more relevant parameter in describing the initiation of the decrease of D because the possibility of forming a ring is roughly proportional to the chain length. Figure 8b gives plots of D/D_0 vs. Here, D_0 is the D of each neat S4VP. As seen in Figure 8b, the decrease of D of both S4VP3 and S4VP4 starts at $\gamma \cong 6$. The D for S4VP1 does not decrease up to $\gamma \cong 6$. Unfortunately, we could not increase the coordination of $CdCl_2$ more than $\gamma \cong 6$ because of the precipitation of some of added $CdCl_2$ was observed for $\gamma > 6$.

Interestingly, D with smaller γ ($\sim$1) was larger than that of neat S4VP1. This behavior might be due to the random positioning of $CdCl_2$ at the coordination site in P4VP blocks nearby junction point of S4VP, which increases the intrinsic correlation length of a coordinated block copolymer. However, as the amount of $CdCl_2$ was further increased, D decreased gradually. This is attributed to the fact that P4VP chains in S4VP1 would be more entangled similar to S4VP3 or S4VP4 resulting from the increased number of the intermolecular coordination. Especially, this trend was more obvious for S4VP1 having shorter chain length compared with S4VP3 and S4VP4. This might be related to the possibility of forming loops.

We also confirmed by TEM that the lamellar microdomains of S4VP1 at 200 °C remained up to $\gamma \cong 6$, as shown in Figure 9. On the other hand, the decrease in D for highly coordinated block copolymer systems produces strong disturbance in the chain conformation; thus, the formation of well-ordered lamellar phases is prohibited, as seen in Figure 10. Such distorted and irregular phase-separated domains would be attributed to

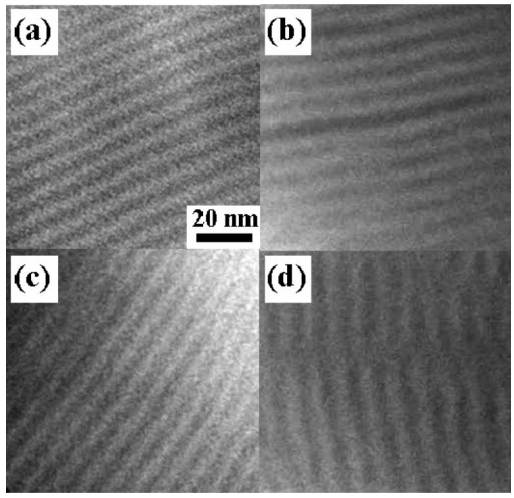

Figure 9. TEM images for (a) neat S4VP1, (b) S4VP1[0.05], (c) S4VP1[0.15], and (d) S4VP1[0.2].

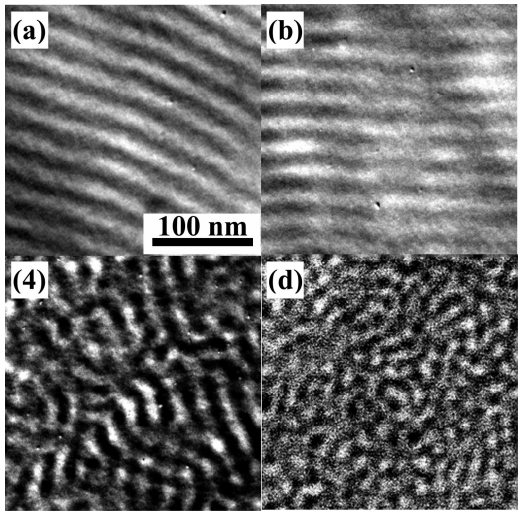

Figure 10. TEM images for (a) neat S4VP3, (b) S4VP3[0.03], (c) S4VP3[0.05], and (d) S4VP3[0.1].

physical gelation which prevents the diffusion of individual chains to form well-organized microdomains. The random sticking of $CdCl_2$ onto P4VP blocks produces irregular phase-separated domains, which induces a partial mixing of PS and P4VP segments nearby junction points of S4VP. Therefore, the interface formed by the S4VP junctions becomes more wiggled at/above gelation point where the phase separation occurs only by local arrangement of the segments within a cluster rather than by entire chain motion, as shown in Figure 10d.

Theoretically, the gelation point can be obtained by the following theoretical approach. For a model system, we consider a mixture of symmetric AB diblock copolymers each with $2N$ monomers and monomeric cross-linkers capable of linking pairs of A-monomers via forming nonpermanent physical bonds. The addition of cross-linkers to the block copolymer gives rise to the formation of (l, m) cluster consisting of l block copolymers and m bonds. Following mean-field cluster theories developed in earlier works,[41–43] the number fraction of (l, m) cluster, $\nu_{l,m}$, is given by

$$\nu_{l,m} = \mathrm{e}^{(l+m-1)-m\beta f_0+\ln\Omega_{l,m}}(\nu_{1,0})^l(\nu_{0,1})^m = \mathrm{e}^{-1}\Omega_{l,m}\xi^l\eta^m \qquad (1)$$

where the f_0 can be interpreted as an effective free energy associated with linking a pair of A-monomers involving the free energy of a physical bond as well as an entropy reduction due to linking A-monomers, $\Omega_{l,m}$ is the number of ways of constructing (l, m) cluster (made of l indistinguishable polymers having N distinguishable functionalities and m indistinguishable cross-linkers), $\nu_{1,0}$ and $\nu_{0,1}$ are the number fractions of free block copolymers and free cross-linkers, respectively, and ξ and η relates to $\nu_{1,0}$ and $\nu_{0,1}$ by $\xi = e\nu_{1,0}$ and $\eta = \mathrm{e}^{-(\beta f_0+1)}\nu_{0,1}$. The exact expression of $\Omega_{l,m}$ is very complicated due to the possibility of ring formation affected by spatial or topological restriction along the chain contour. Here, the "ring closure" refers to a linking which results in any form of local or nonlocal closed structure and is not restricted to the intramolecular head-to-tail linking. Thus, the ring closure can occur in either of two ways: intrachain linking between two pyridine rings belonging to the same chain and multiple interchain linking between a pair of 4VP blocks. However, $\Omega_{l,m}$ can be approximated by introducing a parameter λ that is the probability of the ring closure:[44]

$$\Omega_{l,m} = \frac{N^l(Nl-l)!}{l!(m-l+l)!(Nl-2m)!}\left[\frac{\lambda N}{(Nl-2l+2)}\right]^{m-l+1} \qquad (2)$$

The relation $m = l - 1$ should hold if ring closure is prohibited and $\Omega_{l,m}$ for $m = l - 1$ reduces to Stockmayer's well-known formulation for cross-linked system without ring closure.[45] Any (l, m) clusters with $m > l - 1$ possess more than one ring closure. The parameter λ controls ring closure by $\lambda N = \sigma/\kappa$, where σ is the mean number of available chain points for a single ring closure and κ is the mean number of monomers in a loop. The limit of small λ corresponds to the prohibition of ring formation, whereas the value $\lambda \sim 1$ corresponds to the case that there are no spatial restriction in forming ring closure. Before gelation, the volume fraction of cross-linker (φ) and block copolymer ($1 - \varphi$) should hold in the following equations:

$$\varphi = \frac{p}{2+p} = \nu_{0,1} + \sum_{l=1}^{\infty}\sum_{m=l-1}^{\infty} m\nu_{l,m} = \eta\mathrm{e}^{1+\beta f_0} + \eta\left(\frac{\partial\sum_{l=1}^{\infty}\sum_{m=l-1}^{\infty}\nu_{l,m}}{\partial\eta}\right)_{\varphi,T}$$

$$1-\varphi = \frac{2}{2+p} = \sum_{l=1}^{\infty}\sum_{m=l-1}^{\infty} 2N\nu_{l,m} = 2N\xi\left(\frac{\partial\sum_{l=1}^{\infty}\sum_{m=l-1}^{\infty}\nu_{l,m}}{\partial\xi}\right)_{\varphi,T} \qquad (3)$$

Using eqs 1−3, the gelation point p_{gel} (or φ_{gel}) is obtained. Since our system should consider a gelation of a molten block copolymer where the coordination sites are randomly distributed along the chain, the ring closure concept should be introduced to explain our experimental results. It is noted that the classical gelation theories do not imply the ring closure limit.[45] To consider the effect of the ring formation on gelation behavior, one should include three major parameters: blocky sequence of the coordination sites, the architecture, and steric hindrance. Although our theoretical approach does not take into account the above parameters *explicitly*, these factors are *implicitly* merged in the molecular parameter of λ to describe the tendency of ring closure. This is because λ contains comprehensively information on the mean size of the ring, the mean number of available chain points for a single ring, and steric effects.

Figure 11 shows the theoretically calculated value of γ_{gel} (which is γ at the gel point) as a function of λ for three S4VPs samples. For the calculation, we used $f_0 \approx -155$ kJ/mol (i.e., $\beta f_0 \approx -18710/T$ estimated in ref 46) and found that γ_{gel} is nearly independent of temperature at 100−300 °C. It is noted that the γ_{gel} becomes unity as long as the ring formation is not involved in the cross-linking process. In our system, however, the gelation

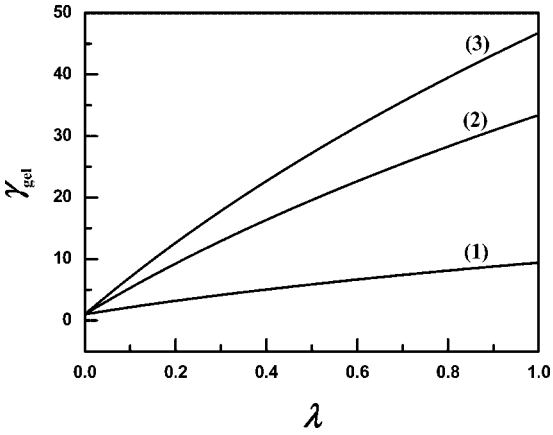

Figure 11. Plot of the gelation point (γ_{gel}) vs λ for (1) S4VP1, (2) S4VP3, and (3) S4VP4.

point turns out to be much larger than unity. For instance, a measurement of the gelation point via TEM and SEM images shows $\gamma_{gel} = 4-6$ for S4VP3. Using the theoretical curve shown in Figure 11, λ is estimated to be ~0.1 for S4VP3. Thus, the possibility of the ring closure might lead to $\gamma_{gel} > 1$. It is also seen in Figure 11 that γ_{gel} is higher for a longer chain, and this trend becomes pronounced as λ increases. This suggests that ring closure is very likely to occur in longer chains compared with shorter chains.

4. Conclusions

In this study, we investigated the effect of $CdCl_2$ on the T_{ODT} and D of S4VP by using shear rheometry, SAXS, and TEM. We found that the addition to $CdCl_2$ significantly increased the T_{ODT} of S4VP. Accordingly, lamellar microdomains could be induced even for an S4VP exhibiting fully disordered state over the entire temperature range by the coordination.

We also studied the change of D of symmetric S4VP with amount of $CdCl_2$. At a relatively low content of $CdCl_2$, D remained nearly constant. However, when the amount of $CdCl_2$ increases further ($\gamma > 6$), D begins to decrease due to the formation of ring structures. It is also found that the scaled gelation point γ_{gel} increases as the molecular weight of block copolymer increases.

Acknowledgment. This work was supported by the National Creative Research Initiative Program by KOSEF. Small-angle X-ray scattering (4C1 and 4C2) was performed at PLS beamline supported by POSCO and KOSEF.

Supporting Information Available: Figures of gel permeation chromatography for neat S4VP1 and S4VP1[0.01], temperature dependence of depolarized light intensity for neat S4VP1, S4VP1[0.003], S4VP1[0.004], S4VP1[0.005], S4VP1[0.01], and S4VP1[0.02], depolarized light intensity and SAXS profiles for S4VP1[0.01] and G' for S4VP1[0.005] during heating and cooling, SAXS profiles for neat S4VP1, S4VP1[0.01], and polyimide windows. This material is available free of charge via the Internet at http://pubs.acs.org.

References and Notes

(1) Helfand, E.; Wasserman, Z. R. In *Developments in Block Copolymer*; Goodman, I., Ed.; Applied Science: New York, 1982.
(2) Hashimoto, T. In *Termoplastic Elastomers*; Legge, N. R., Holden, G., Schroeder, H. E., Eds.; Hanser: New York, 1987.
(3) Hamley, I. W. *The Physics of Block Copolymers*; Oxford University Press: New York, 1998.
(4) Leibler, L. *Macromolecules* **1980**, *13*, 1602.
(5) Bates, F. S.; Fredrickson, G. H. *Annu. Rev. Phys. Chem.* **1990**, *41*, 525.
(6) Matsen, M. W.; Bates, F. S. *Macromolecules* **1996**, *29*, 1091.
(7) Hasegawa, H.; Tanaka, H.; Yamasaki, K.; Hashimoto, T. *Macromolecules* **1987**, *20*, 1651.
(8) Almdal, K.; Rosedale, J. H.; Bates, F. S.; Wignall, G. D.; Fredrickson, G. H. *Phy. Rev. Lett.* **1990**, *65*, 1112.
(9) Ribbe, A. E.; Okumura, A.; Matsushige, K.; Hashimoto, T. *Macromolecules* **2001**, *34*, 8239.
(10) Lin, Y.; Böker, A.; He, J.; Sill, K.; Xiang, H.; Abetz, C.; Li, X.; Wang, J.; Emrick, T.; Long, S.; Wang, Q.; Balaz, A.; Russell, T. P. *Nature (London)* **2005**, *434*, 55.
(11) Agnew, N. H. *J. Polym. Sci.* **1976**, *14*, 2819.
(12) Haryono, A.; Binder, W. H. *Small* **2006**, *2*, 600.
(13) Zhao, H.; Oduglas, E. P.; Harrison, B. S.; Schanze, K. S. *Langmuir* **2001**, *17*, 8428.
(14) Chiu, J. J.; Kim, B. J.; Kramer, E. J.; Pine, D. J. *J. Am. Chem. Soc.* **2005**, *127*, 5036.
(15) Yeh, S. W.; Wei, K. H.; Sun, Y. S.; Jeng, U. S.; Liang, K. S. *Macromolecules* **2005**, *38*, 6559.
(16) Förster, S.; Antonietti, M. *Adv. Mater.* **1998**, *10*, 195.
(17) Lo, C. T.; Lee, B.; Winans, R. E.; Thiyagarajan, P. *Macromolecules* **2006**, *39*, 6318.
(18) Ruokolainen, J.; Mäkinen, R.; Torkkeli, M.; Mäkelä, T.; Serimaa, R.; ten Brinke, G.; Ikkala, O. *Science* **1998**, *280*, 557.
(19) Ruokolainen, J.; ten Brinke, G.; Ikkala, O. *Adv. Mater.* **1999**, *11*, 77.
(20) Bondizic, A.; de Wit, J.; Polushkin, E.; Schouten, A. J.; ten Brinke, G.; Ruokolainen, J.; Ikkala, O.; Dolbnya, I.; Bras, W. *Macromolecules* **2004**, *37*, 9517.
(21) Schultz, M. F.; Khandpur, A. K.; Bates, F. S.; Almdal, K.; Mortensen, K.; Hajduk, D. A.; Gruner, S. M. *Macromolecules* **1996**, *29*, 2857.
(22) Schultz, M. F.; Bates, F. S.; Almdal, K.; Mortensen, K. *Phys. Rev. Lett.* **1994**, *73*, 86.
(23) Shull, K. R.; Kramer, E. J.; Hadziioannou, G.; Tang, W. *Macromolecules* **1990**, *23*, 4780.
(24) Rukolainen, J.; Torkkeli, M.; Serimaa, R.; Komanschek, E.; ten Brinke, G.; Ikkala, O. *Macromolecules* **1997**, *30*, 2002.
(25) Han, S. H.; Lee, D. H.; Kim, J. K. *Macromolecules* **2007**, *40*, 7416.
(26) Zha, W.; Han, C. D.; Lee, D. H.; Han, S. H.; Kim, J. K.; Kang, J. H.; Park, C. *Macromolecules* **2007**, *40*, 2109.
(27) Ruzette, A. V.; Soo, P. P.; Sadoway, D. R.; Mayes, A. M. *J. Electrochem. Soc.* **2001**, *148*, A537.
(28) Epps, T. H., III; Bailey, T. S.; Pham, H. D.; Bates, F. S. *Chem. Mater.* **2002**, *14*, 1706.
(29) Epps, T. H., III; Bailey, T. S.; Waletzko, R.; Bates, F. S. *Macromolecules* **2003**, *36*, 2873.
(30) Wang, J.; Leiston-Belagner, J. M.; Sievert, J. D.; Russell, T. P. *Macromolecules* **2006**, *39*, 8487.
(31) Wang, J.; Chen, W.; Roy C.; Sievert, J. D.; Russell, T. P. *Macromolecules* **2008**, *41*, 963.
(32) Lee, D. H.; Kim, H. Y.; Kim, J. K.; Huh, J.; Ryu, D. Y. *Macromolecules* **2006**, *39*, 2027.
(33) Ryu, D. Y.; Jeong, U.; Lee, D. H.; Kim, J.; Youn, H. S.; Kim, J. K. *Macromolecules* **2003**, *36*, 2894.
(34) Bates, F. S.; Rosadale, J. H.; Fredrickson, G. H. *J. Chem. Phys.* **1990**, *92*, 6255.
(35) (a) Han, C. D.; Kim, J.; Kim, J. K. *Macromolecules* **1989**, *22*, 383. (b) Han, C. D.; Baek, D. M.; Kim, J. K. *Macromolecules* **1990**, *23*, 561.
(36) Han, C. D.; Baek, D. M.; Kim, J. K.; Ogawa, T.; Sakamoto, N.; Hashimoto, T. *Macromolecules* **1995**, *28*, 5043.
(37) Hahn, H.; Eitouni, H. B.; Balsara, N. P.; Pople, J. A. *Phys. Rev. Lett.* **2003**, *90*, 155505.
(38) Hahn, H.; Chakraborty, A. K.; Das, J.; Pople, J. A.; Balsara, N. P. *Macromolecules* **2005**, *38*, 1277.
(39) Gomez, E. D.; Das, J.; Chakraborty, A. K.; Pople, J. A.; Balsara, N. P. *Macromolecules* **2006**, *39*, 4848.
(40) Durkee, D. A.; Gomez, E. D.; Ellsworth, M. W.; Bell, A. T.; Balsara, N. P. *Macromolecules* **2007**, *40*, 5103.
(41) Tanaka, F. *Macromolecules* **1990**, *23*, 3790.
(42) Angerman, H. J.; ten Brinke, G. *Macromolecules* **1999**, *32*, 6813.
(43) Huh, J.; Jo, W. H. *Macromolecules* **2004**, *37*, 3037.
(44) Harris, F. E. *J. Chem. Phys.* **1955**, *23*, 1518.
(45) Stockmayer, W. H. *J. Chem. Phys.* **1943**, *11*, 45.
(46) Sawada, K.; Satoh, K.; Shirakura, Y.; Masuda, Y. *Bull. Chem. Soc. Jpn.* **2001**, *74*, 1285.

MA702403K